# Differential specific radiation damage in the Cu(II)- and Pd(II)-bound forms of an α-helical foldamer: a case study of crystallographic phasing by RIP and SAD

Klaus Fütterer,[a]* Raimond B.G. Ravelli,[b] Scott A. White,[a] Andrew J. Nicoll,[c,d] Rudolf K. Allemann[c]

[a] School of Biosciences, University of Birmingham, Edgbaston, Birmingham, B15 2TT, UK; [b] EMBL, 6 rue Jules Horowitz, BP 181, 38042 Grenoble CEDEX 9, France, [c] School of Chemistry, Cardiff University, Main Building, Park Place, Cardiff, CF10 3AT, UK;
[d] Present address: MRC Prion Unit, Department of Neurodegenerative Disease, Institute of Neurology, Queen Square, London, WC1N 3BG, UK.

Email correspondence: K.Futterer@bham.ac.uk

## Supplementary Tables and Figures

## Supplementary Table 1

Complete statistics of X-ray diffraction data mentioned in the main text. Numbers in parentheses refer to the last resolution shell.

| | Cu-MINTS | | Pd-MINTS (*Mpd7)* | | | | Pd-MINTS (*Mpd3*) | Pd-MINTS (*Mpd1*) |
|---|---|---|---|---|---|---|---|---|
| | Before | After | Before | Middle | After1 | After2 | SAD | SAD |
| Station [a)] | ID14-4 | ID14-4 | ID14-4 | ID14-4 | ID14-4 | ID14-4 | in-house | ID29 |
| Wavelength (Å) | 0.97857 | 0.97857 | 0.93926 | 0.93926 | 0.93926 | 0.93926 | 1.54178 | 0.97925 |
| Space group | $P6_322$ | | $P4_12_12$ | | | | $P4_12_12$ | $P4_12_12$ |
| a, b (Å) | 44.35 | 44.40 | 30.45 | 30.46 | 30.49 | 30.49 | 30.40 | 30.19 |
| c | 58.36 | 58.48 | 48.12 | 48.14 | 48.14 | 48.15 | 48.17 | 50.23 |
| Resolution limits | 38.4-1.10 | 38.46-1.2 | 48.1-1.1 | 48.1-1.1 | 48.11-1.1 | 48.2-1.1 | 19.63-1.91 | 30.19-1.31 |
| (last shell) | (1.16-1.10) | (1.27-1.2) | (1.16-1.10) | (1.16-1.10) | (1.16-1.10) | (1.16-1.10) | (2.01-1.91) | (1.38-1.31) |
| Rmerge (%)[b)] | 10.3(36.4) | 9.8(60.3) | 5.4(23.4) | 5.5(28) | 5.6(34.7) | 6.1(43.7) | 4.4(7.7) | 5.9(22.8) |
| No. of observations | 471044(65124) | 119843(13483) | 71236(10066) | 71288(10133) | 71402(10099) | 71443(10113) | 11850(1221) | 153297(17711) |
| No. of unique reflections | 14358(2027) | 11186(1560) | 9757(1387) | 9758(1390) | 9766(1383) | 9769(1381) | 1990(270) | 6030(845) |
| Mean((I)/sd(I)) | 28.1(10.2 | 14.4(3.2) | 21.4(7.3) | 20.9(6.2) | 20(5.1) | 18.4(4.1) | 30.3(18.5) | 43.2(15) |
| Completeness (%) | 99.8(99.2) | 99.7(98.1) | 99.9(99.8) | 100(100) | 99.9(99.8) | 100(99.9) | 99.5(97.7) | 99.8(99.1) |
| Multiplicity | 32.8(32.1) | 10.7(8.6) | 7.3(7.3) | 7.3(7.3) | 7.3(7.3) | 7.3(7.3) | 6(4.5) | 25.4(21) |
| Anom. completeness (%) | 99.7(98.5) | 99.7(97.8) | 99.9(99.2) | 100(99.8) | 99.9(99.5) | 100(99.8) | 98.4(89.8) | 99.9(99.3) |
| Anom. multiplicity | 17.9(17.1) | 5.8(4.6) | 4(3.9) | 4(3.9) | 4(3.9) | 4(3.9) | 3.6(2.7) | 14.3(11.4) |

[a] Beamlines ID14-4, ID29 are at the ESRF, Grenoble, France. The in-house X-ray source was a MicroMax 007HF generator with VariMax™ confocal optics (Rigaku, The Woodlands, Texas, USA).

[b] Rmerge = $\Sigma_h\Sigma_i | I(h,i) - \langle I(h)\rangle | / \Sigma_h\Sigma_i I(h,i)$, where I(h,i) is the intensity of the ith measurement of reflection h and $\langle I(h)\rangle$ is the mean value of I(h,i) for all i measurements.

## Supplementary Table 2

Heavy atoms sites (fractional coordinates) and statistics of RIP phasing

| **Pd-MINTS** | | | | | |
|---|---|---|---|---|---|
| Residue | Atom | X | Y | Z | Occ |
| Cys-4 | Sγ | 0.728 | 0.875 | 0.109 | 1.00 |
| Cys-8 | Sγ | 0.844 | 0.988 | 0.170 | 1.00 |
| Cys-16 | Sγ | 0.777 | 0.911 | 0.090 | 0.99 |
| Cys-18 | Sγ | 0.849 | 1.043 | 0.146 | 0.95 |
| Asp-1 | Oδ1 | 0.692 | 0.723 | 0.143 | 0.50 |
| MPD-21 | O4 | 0.627 | 0.872 | 0.156 | 0.43 |
| Pd | Pd(II) | 0.816 | 0.816 | 0.000 | 0.40 |
| **Cu-MINTS** | | | | | |
| CuB | Cu(II) | 0.561 | 0.238 | 0.027 | 1.00 |
| CuA | Cu(II) | 0.420 | 0.155 | -0.196 | 0.96 |
| Wat-10 | O | 0.640 | 0.259 | -0.011 | 0.57 |
| Cys-4 (chain B) | Sγ | 0.405 | 0.168 | 0.086 | 0.51 |
| | | | | | |
| **RIP** (*SHELXD/E*) | Cu-MINTS | Pd-MINTS | | | |
| FIND/DSUL | 8/4 | 4/2 | | | |
| Range of scale factor K | 1.000 | 0.900-0.999 | | | |
| High resolution cut-off *SHELXD* (Å) | 1.6 | 1.4 | | | |
| Expanded in *SHELXE* to (Å) | 1.2 | 1.2 | | | |
| K for best CC | - | 0.912 | | | |
| CCbest[a] | 28 | 34.5 | | | |
| CCweak[a] | 14.7 | 23.1 | | | |
| PATFOM | 37.8 | 25.6 | | | |
| Solvent Content | 0.45 | 0.45 | | | |
| K for best pseudo-free CC | - | 0.984 | | | |
| Contrast[b] | 0.68 | 1.13 | | | |
| Connectivity[b] | 0.86 | 0.91 | | | |
| Pseudo-free CC | 83.3 | 88.5 | | | |
| wMPE (º) (38-1.2 Å) | 15.4 | 19.2 | | | |
| Map correlation coefficient | 0.832 | 0.842 | | | |
| **SAD** (*SHARP*) | | | | | |
| wMPE (º) (38-1.2Å) | 28.6 | 31.6 | | | |
| Map correlation coefficient | 0.811 | 0.834 | | | |

[a] Solution from SHELXD with highest CCbest.

[b] Solution from SHELXE with highest pseudo-free CC.

# 1 Legends for Supplementary Figures

### Supplementary Figure S1

SAD density maps of Pd-MINTS contoured at 1.2 σ using data recorded *(a)* in-house of crystal *Mpd3* to 1.9 Å, *(b)* on beamline ID29 of crystal *Mpd1* to 1.3 Å, and *(c)* using the first 50º (100 frames) of the 'Before' data of crystal *Mpd7* to 1.1 Å.

### Supplementary Figure S2

Difference Fourier density (mFo – DFc) around the Cys-8–Cys-18 disulfide bond contoured at +3 σ (blue, cyan) and –3 σ (red, yellow), calculated on the basis of the refined model. Maps were calculated with amplitudes of the 'Before' (blue and red), and 'After' (yellow and cyan) data. Residues are labelled, with subscripts indicating the chain ID in *b), c)* and primes denoting symmetry-related chains. *(a)* Pd-MINTS. *(b,c)* Cu-MINTS.

### Supplementary Figure S3

Difference Fourier map (mFo – DFc) around His-3 in Pd-MINTS using phases from a model that included only a single conformer for this residue.

### Supplementary Figure S4

Ribbon diagram of Pd-MINTS illustrating the crystal packing.

# 2 Supplementary Figures

## Supplementary Figure S1

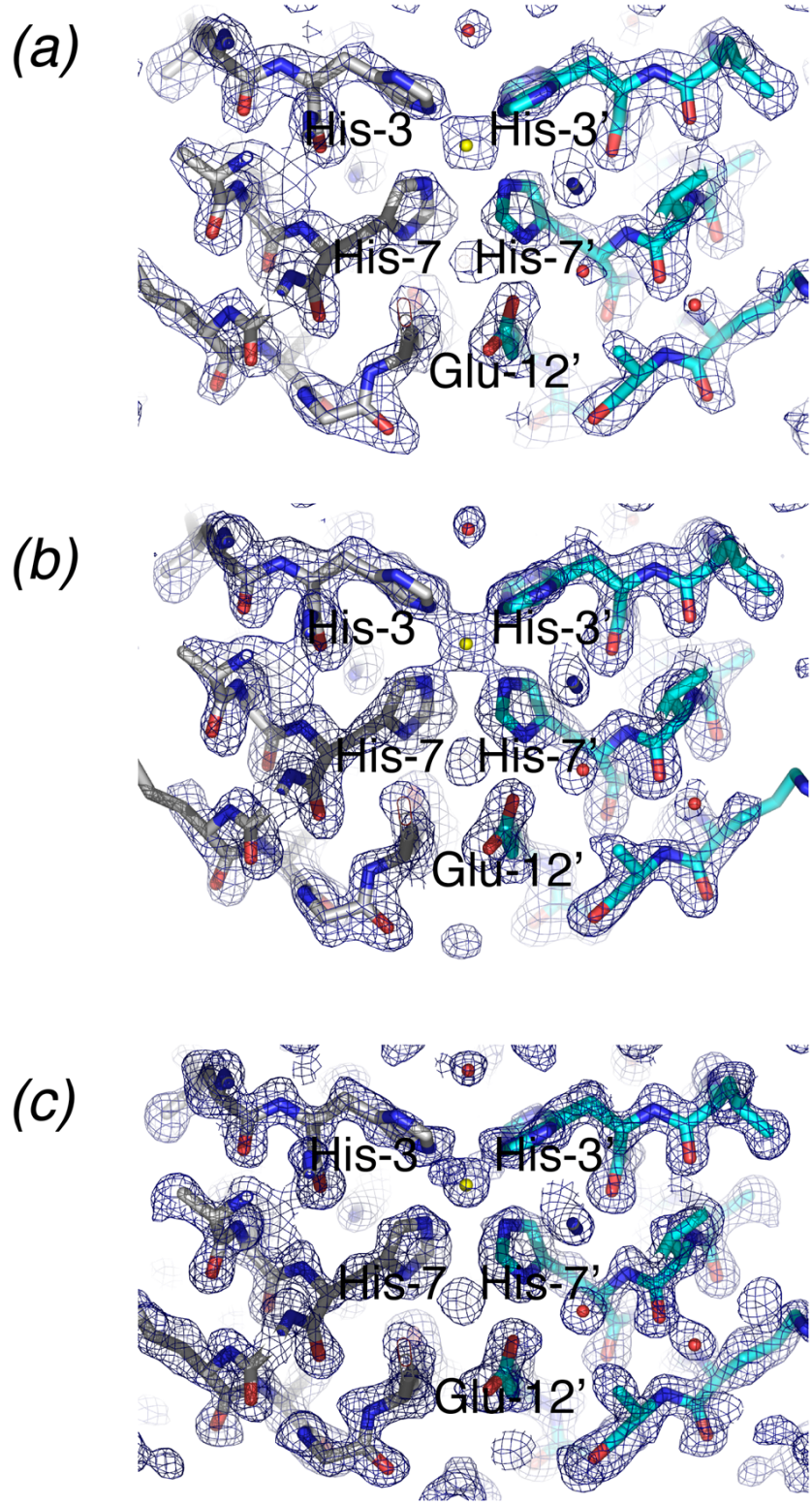

**Supplementary Figure S2**

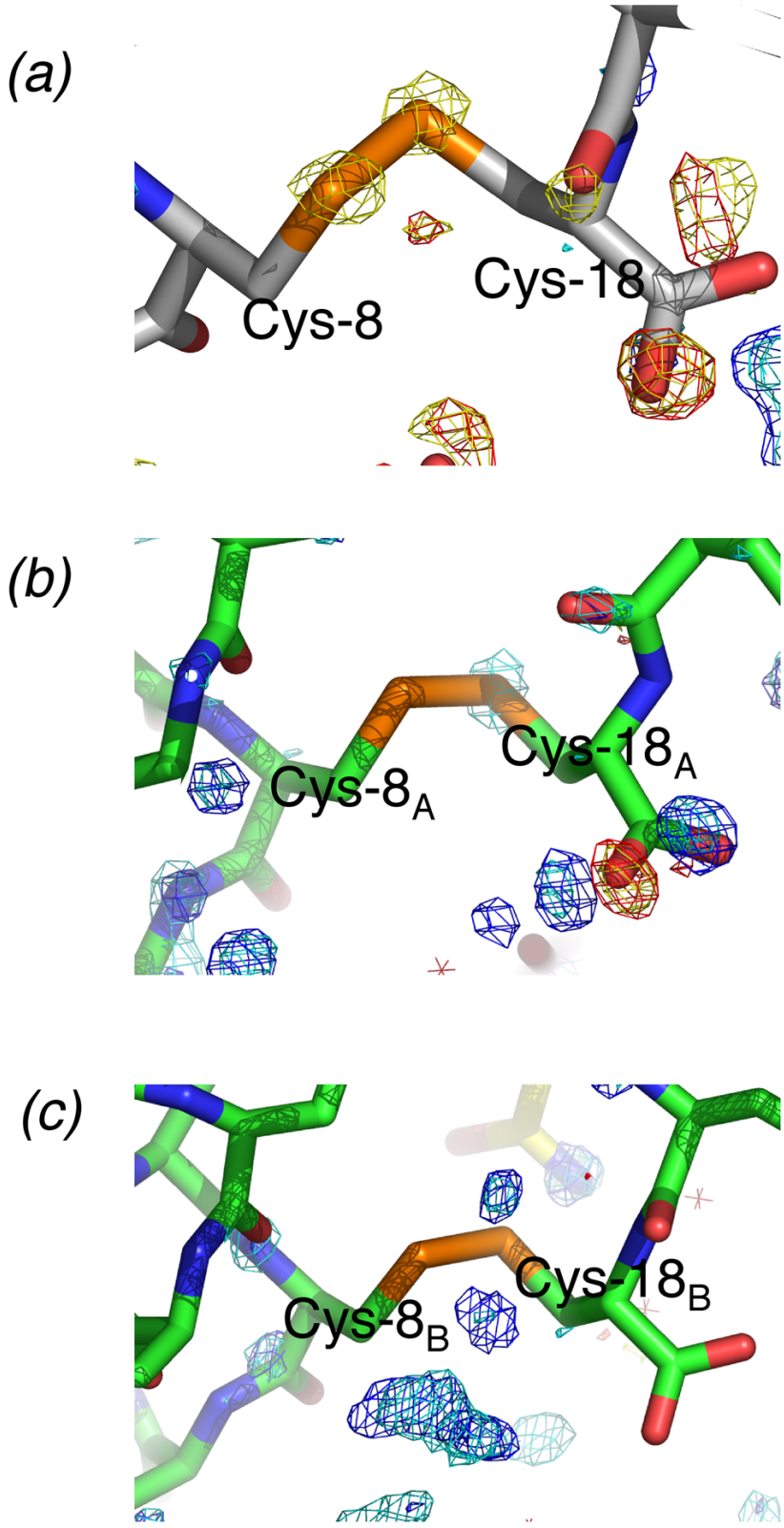

**Supplementary Figure S3**

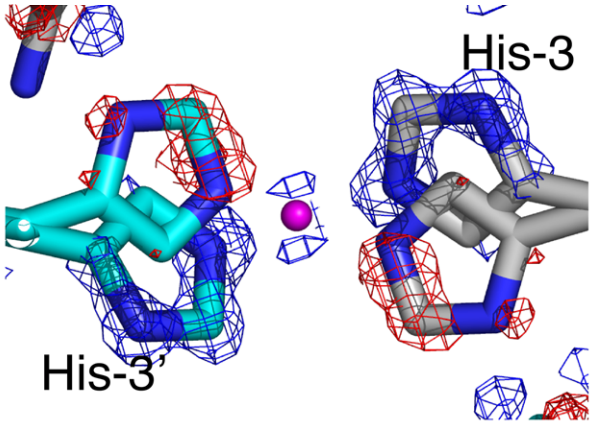


**Supplementary Figure S4**